

# Developing an Insect Odorant Receptor Bioelectronic Nose for Vapour-Phase Detection

by Eddyn Oswald Perkins Treacher

A thesis submitted in partial fulfilment of the  
requirements of the degree of  
Doctor of Philosophy in Physics  
School of Physical and Chemical Sciences  
Te Herenga Waka - Victoria University of Wellington

Dec 2024





# Abstract

The ability to detect volatile organic compounds in a highly sensitive and selective manner is desirable for applications as varied as diagnosis of illnesses at a remote clinic, monitoring of air in an industrial setting, or identification of invasive organisms at a biosecurity checkpoint. Historically, animal noses have been used for such tasks, as their combined sensitivity and selectivity are superior to traditional artificial sensors. However, training and deploying animals in such situations is both time and cost intensive. In recent years, an improved understanding of *in vivo* biological sensing has driven efforts to mimic these highly efficient processes in an artificial sensor format.

To this end, a “bioelectronic nose” was developed. This sensor uses an artificial transducer to amplify responses of an insect odorant receptor protein to specific volatile compounds. Thin-film transistors were used as the amplifier element, given their low cost, small size and extreme sensitivity. Various thin-film morphologies were compared, and their suitability for bioelectronic nose development assessed. Transducers made using a novel steam-assisted thin-film deposition technique were found to have highly consistent device-to-device electrical properties relative to other films. Films made using this process typically showed more surface contamination than other morphologies, but their high sensitivity was nonetheless confirmed with a non-specific sensing series in an aqueous environment.

One of the major challenges encountered in this thesis was variability in the quality of sensor functionalisation. Raman spectroscopy and fluorescence microscopy confirmed an existing non-covalent attachment method could successfully immobilise nanodiscs onto the transistor channel region. However, various sensors functionalised using the same procedure often exhibited no sensing activity. Extensive electrical characterisation indicated the presence of an unidentified contamination layer preventing electrical interaction between the insect odorant receptors and transducer thin-film. It was shown that this layer was unlikely to be directly associated with the thin-film morphology used for the transducer.

Subsequently, an alternative biotin-based non-covalent method was used for functionalisation of the proteins, which eliminated several possible contamination sources. This alternative biotin-based method was used to demonstrate successful aqueous sensing of femtomolar concentrations of methyl salicylate by an iOR10a-functionalised device. When tested in a custom-built vapour delivery system, a similar bioelectronic sensor was shown to be highly sensitive to the target vapour. However, consistent reproduction of the biotin-based method was challenging due to the harsh cleaning method involved. It was therefore difficult to determine conclusively whether sensor responses were selective. By finding new, systematic approaches to address the major barriers to sensor success carefully identified in this work, there are promising signs that a highly reliable vapour-phase bioelectronic nose can be produced.



# Acknowledgements

I would first like to acknowledge the lands of my ancestors, and the lands of the sovereign first peoples to which my ancestors travelled. We each come from the land, live off the land and return to the land.

*Noon of Essex to Warrang, on the Friends, Autumn 1811*

*Cave of Cambridgeshire to Warrang, on the Royal Charlotte, Autumn 1825*

*Boyce of Suffolk to Warrang, 1832*

*Charlton of Northumberland to Warrang, on the Clyde, Spring 1834*

*Prouse of Devonshire to Pito-one, on the Duke of Roxburgh, Summer 1840*

*Ebden of Devonshire to Pito-one, on the Tyne, Winter 1841*

*Collis of Hampshire to Pito-one, on the Birman, Autumn 1842*

*Swann of Loch Garman to Te Whanganui-a-Tara, 1844*

*Blythe of Berkshire to Whakatū, circa 1846*

*Innes of Berkshire to Naarm, on the Sacramento, Autumn 1853*

*Sheppard of Gloucestershire to Naarm, 1853*

*Bruce of London to Naarm, on the Omega, Autumn 1855*

*Quennell of Surrey to Warrang, on the Asiatic, Winter 1855*

*Barr of Glasgow to Kōpūtai, on the Sir Edward Paget, Winter 1856*

*Perkins of London to Te Whanganui-a-Tara, on the Matoaka, Spring 1859*

*McKee of Antrim to Tāmaki Makaurau, on the Indian Empire, Spring 1862*

*Sandilands of Peeblesshire to Ōtepoti, circa 1864*

*Treacher of Berkshire to Te Whanganui-a-Tara, on the Wild Duck, Summer 1865*

*McTaggart of Argyllshire to Kōpūtai, on the Edward P. Bouverie, Autumn 1869*

*Chapman of Kent to Whakatū, on the Adamant, Winter 1874*

*Cheel of London to Whakatū, on the Queen Bee, Winter 1877*

*Hutchison of Aberdeen to Tarntanya, before 1882.*

I chose to start my doctoral studies just a few months into a global pandemic. Completing a challenging project with a worldwide crisis in the background might have been impossible without the supervision of AProf. Natalie Plank. Her ability to adapt to and overcome any problem has taught me that there is no situation which is truly unmanageable. I am deeply grateful for her leadership throughout a time of particular chaos.

## *Acknowledgements*

I started this project with minimal formal training in biological science, coming from a primarily physics and engineering background.

The immense support I received from Melissa Jordan and Colm Carraher from the Institute for Plant and Food Research (PFR) to complete this project meant that this was not an issue, and I thank them both immensely for this.

I would not have been able to begin this thesis without the financial backing and support I received from PFR and the Better Border Biosecurity (B3) programme. In particular, I am very grateful to Andrew Kralicek, formerly with PFR and now at Scentian Bio, and the ex-Director of B3, David Teulon, for helping to secure funding for my project. I would also like to thank the donor of the Ernest Marsden Scholarship in Physics for their significant financial support.

There are many incredibly supportive people who I worked alongside during my project. I would like to start off by thanking Rifat Ullah, whose mentoring and kindness encouraged me to pursue further study. His work on the initial design and setup of the vapour delivery system was invaluable to me throughout this project. I am also especially grateful to Alex Puglisi, for constructing the mechanical elements of the vapour delivery system and giving me extensive feedback on the system design. I would like to thank Peter Coard, for his advice and guidance when constructing the electrical elements of the vapour delivery system. I thank Selvan Murugathas, too, for his advice on constructing the insect odorant receptor sensors, as well as Damon Colbert and Valentina Lucarelli, who provided the insect odorant receptor nanodiscs used in this work.

Thank you to AProf. Ben Ruck, my supportive secondary supervisor, and to AProf. Franck Natali, for always asking about my thesis in the tearoom. Thank you to Gideon Gouws for his friendly encouragement and advice. For their substantial technical assistance and mentoring during this project, I thank Alan Rennie, Grant Franklin, Chris Lepper, Rashika Gunasekara, Pete Jebson and Sushila Pillai from VUW, Andrew Chan from PFR, AProf. Charles Unsworth from the University of Auckland, and Prof. Simon Brown and his nanomaterials group from the University of Canterbury.

I was lucky enough to start my doctoral program just as a group of supportive and talented senior students were finishing, and finished just as a group of enthusiastic and talented new doctoral students were starting. A special thanks to Jenna Nyugen, Erica Happe and Erica Cassie for teaching me the fabrication processes and characterisation procedures that made this thesis happen; and a special thanks to Marissa Dierkes, Danica Fontein, Sangar Begzaad and Alireza Zare, for their incredible support throughout the thesis writing process. I am also thankful for the assistance of the cleanroom group interns over the course of my PhD, including Liam, Hayden and Lotte. I would further like to thank everyone else I shared an office with and worked alongside, including Jackson, Will, Roshni, Ali, Sam, Kira, Catherine, Martin, Janani, Ted, Kiri and Joe.

A massive thank you to Openstar Technologies. It has been an honour to work on a cutting-edge plasma physics project right here in Te Whanganui-a-Tara. A particularly big thank you to Ratu, Darren and Thomas for having me as part of the plasma

### *Acknowledgements*

physics team. Thank you also to the other Openstar interns, in particular the other plasma physics interns, Valentina, Benjy and Chris. I wish you success in all your dipole-confined plasma related endeavours.

I want to thank Shodokan Aikido New Zealand for their support throughout this thesis, in particular for the once-in-a-lifetime opportunity to travel to Osaka to be graded for first-dan by Nariyama Shihan. Thanks for all the training and support, Ian. Thank you to all the friends and family, old and new, who have supported me over these wild past few years. You know who you are.

Thank you to my brother, Keeson, and to my parents, Hilary and Phillip. Your support means everything to me, and I would not be where I am today without you. Our Friday lunchtime cafe visits inspired and motivated me throughout the doctoral program. Thank you, thank you, thank you for your love, your compassion, and for being there for me.

Finally, thank you Nina. Your love has kept me going through the most difficult and most wonderful times over the last three and a half years. You are the light of my life, and I am so happy to have taken on this challenge with you by my side.

Arohanui and peace to you all, Eddyn (Ned)



# **Table of Contents**



## List of Figures



## List of Tables



# List of Abbreviations

2D	2-Dimensional
Ab	Antibody
AB	Amyl Butyrate
AB-NTA	Na, $\text{Na}$ -Bis(carboxymethyl)- <i>L</i> -lysine hydrate
AFM	Atomic Force Microscope/Microscopy
AH	Absolute Humidity
Avi-tag	Avidin-tag
BMIM	1-butyl-3-methylimidazolium bis(trifluoromethylsulfonyl)imide
BWF	Breit-Wigner-Fano
CAD	Computer Aided Design
CNT	Carbon Nanotube
CVD	Chemical Vapour Deposition
Cy3	Cyanine 3
DAN	1,5-diaminonaphthalene
DAQ	Data Acquisition Input/Output Module
DCB	1,2-dichlorobenzene
DI	Deionised
DMF	Dimethylformamide
DMSO	Dimethylsulfoxide
DMT-MM	4-(4,6-dimethoxy-1,3,5-triazin-2-yl)-4-methylmorpholinium chloride
DMMP	Dimethyl Methylphosphonate
DNA	Deoxyribonucleic Acid
E2Hex	<i>trans</i> -2-hexan-1-al
EB	Ethyl Butyrate
EDC	1-Ethyl-3-(3-dimethylaminopropyl)carbodiimide
EDL	Electric Double Layer
EIS	Electrochemical Impedance Spectroscopy
EtHex	Ethyl Hexanoate

*List of Abbreviations*

EtOH	Ethanol
FET	Field-Effect Transistor
FITC	Fluorescein isothiocyanate
GA	Glutaraldehyde
GFET	Graphene Field-Effect Transistor
GFP	Green Fluorescent Protein
GPCR	G-protein Coupled Receptor
HEK	Human Embryonic Kidney
His-tag	Histidine-tag
hOR	Human Odorant Receptor
HPLC	High-performance Liquid Chromatography
iOR	Insect Odorant Receptor
IPA	Isopropanol
LOD	Limit of Detection
m-CNT	Metallic Carbon Nanotube
MeOH	Methanol
MeSal	Methyl Salicylate
MFC	Mass Flow Controller
mOR	Mouse Odorant Receptor
MOSFET	Metal-Oxide-Semiconductor Field-Effect Transistor
MSP	Membrane Scaffold Protein
MWCNT	Multi-Walled Carbon Nanotube
ND	Nanodisc
NHS	N-Hydroxysuccinimide
NHSS	N-hydroxysulfosuccinimide
NMR	Nuclear Magnetic Resonance
NSB	Non-Specific Binding
NTA	Nitrilotriacetic Acid
OBP	Odorant Binding Protein
OR	Odorant Receptor
ORCO	Odorant Receptor Co-Receptor

*List of Abbreviations*

PBA	1-Pyrenebutyric Acid
PBASE	1-Pyrenebutanoic Acid N-hydroxysuccinimide Ester
PBS	Phosphate-Buffered Saline
PCB	Printed Circuit Board
PDL	Poly- <i>D</i> -lysine
PDMS	Polydimethylsiloxane
PEG	Polyethylene Glycol
PID	Photoionisation Detector
PLL	Poly- <i>L</i> -lysine
PPB	Pyrene-PEG-Biotin
PPF	Pyrene-PEG-FITC
PPN	Pyrene-PEG-NTA
PPR	Pyrene-PEG-Rhodamine
PTFE	Polytetrafluoroethylene (Teflon <sup>TM</sup> )
PVC	Polyvinyl chloride
QCM	Quartz Crystal Microbalance
RH	Relative Humidity
RHI	Relative Humidity and Temperature Indicator
RNA	Ribonucleic Acid
SAW	Surface Acoustic Wave
s-CNT	Semiconducting Carbon Nanotube
SEM	Scanning Electron Microscope/Microscopy
SMU	Source Measure Unit
SPR	Surface Plasmon Resonance
SWCNT	Single-Walled Carbon Nanotube
TFTFET	Thin-Film Field-Effect Transistor
TMAH	Tetramethylammonium hydroxide
TX	Transfer Characteristics
UV	Ultraviolet
VI	Virtual Instrument
VUAA1	N-(4-Ethylphenyl)-2-[4-ethyl-5-(pyridin-3-yl)-4H-1,2,4-triazol-3-yl]sulfanylacetamide



# 1 Introduction

## 1.1 Background

The ‘bioelectronic nose’, an electronic transducer modified with elements of the animal olfactory system, has the potential to allow specific detection of airborne volatile compounds at concentrations as low as parts per trillion [Glatz2011, Kwon2015, Dung2018, Kim2022a]. An ideal transducer platform is the thin-film transistor (TFT) which is particularly portable, simple to use, small and robust [Kauffman2008, Khan2020]. The thin films used in these field-effect transistors (FETs) include carbon nanotube networks and graphene, low-dimensional nanomaterials which are both highly sensitive and biocompatible [Shkodra2021]. The implications of successful development of such a portable and robust bioelectronic nose are significant. Applications could be found in high-importance fields such as biosecurity, medicine, environmental protection and food safety [Dung2018, Arakawa2019, Yang2017, Son2017]. For example, it has been demonstrated that it is possible to detect invasive brown marmorated stinkbugs based on their volatile trace [Moser2020]. A bioelectronic nose could potentially accomplish this biosecurity task far more cheaply and efficiently than trained sniffer dogs [Lee2010, Moon2020, Terutsuki2020]. There has been rapid progress in the development of bioelectronic noses using carbon nanotube field-effect transistors (CNT FETs) and graphene field-effect transistors (GFETs) over the past 15-20 years [Yoon2009, Lee2010, Yang2018].

Insect odorant receptors (iORs) enable simple invertebrates, such as the vinegar fruit fly *Drosophila melanogaster*, to distinguish between a huge number of specific volatile compounds [Hallem2004, Smart2008, Wicher2008, Munch2016, Bohbot2020]. Within the past five years, a variety of *Drosophila melanogaster* iORs have been successfully coupled with highly sensitive low-dimensional thin-film transistors (TFTs) for specific detection of fruit-like odors in an aqueous environment [Murugathas2019a, Murugathas2020]. iORs have also been used for sensitive and selective volatile detection in a lipid bilayer format, but not in a portable bioelectronic nose format [Yamada2021]. In this thesis, my aim was to investigate whether a bioelectronic nose capable of odorant detection in a vapour-phase environment could be constructed by coupling iORs with TFTs. Alongside practical applications, development of a vapour-phase bioelectronic nose using iORs may give us a greater understanding of the mechanisms underlying insect olfaction [Lee2010]. The transduction mechanism of nanomaterial-based iOR sensors is still unknown, and I hope to shed further light on the

## 1 Introduction

biological and electronic processes underpinning this mechanism [**Murugathas2020**, **Khadka2019**, **Cheema2021**].

### 1.2 Thesis Outline

This thesis consists of nine chapters. The first three chapters, including this one, are background chapters introducing the general topics of this thesis. The fourth and fifth chapters are methods chapters, while the next three chapters (sixth, seventh and eighth) describe the results obtained. The ninth chapter concludes the thesis and discusses possible next steps for future research.

**Chapter 2** gives a broad description of carbon nanotube and graphene field-effect transistors with a focus on their use in sensing applications. The chapter begins by looking at the general structure and properties of thin-film transistors, where key figures of merit such as transconductance, on-off ratio, gate current and hysteresis are described. Graphene field-effect transistors (GFETs) and carbon nanotube network field-effect transistors (CNT FETs) are then discussed in greater detail. These descriptions include the chemical composition of each nanomaterial, their conduction behaviour and their unique sensor properties when integrated into a field-effect transistor as a thin-film.

**Chapter 3** investigates existing odorant receptor-coupled thin-film field-effect transistors in the literature. First, the biological structure of odorant receptors and membrane formats for their protection *in vitro* are discussed. Details are then provided regarding the construction and operation of existing vertebrate odorant receptor TFT biosensors. The structure and function of the insect odorant receptor is then contrasted with the vertebrate odorant receptor, and existing insect odorant receptor TFT biosensors in the literature are discussed. The chapter finishes with a brief discussion of non-specific binding and its role in hindering biosensor activity.

**Chapter 4** describes the fabrication of the CNT FET and GFET transducers used in this thesis and the characterisation techniques used to probe their behaviour. The chapter starts with an introduction to photolithography for thin-film transistor device fabrication. Various techniques are described for random deposition of carbon nanotube networks to act as channels for these thin-film transistors. Characterisation techniques described in this chapter include atomic force microscopy (AFM), fluorescence microscopy, Raman spectroscopy and electrical characterisation with various semiconductor device analysers.

**Chapter 5** presents the results obtained from the use of characterisation techniques on the pristine GFETs and CNT FETs. Various carbon nanotube (CNT) network morphologies are displayed and analysed. The Raman spectra and electrical device parameters of these CNT network morphologies are then discussed, along with electrical parameters from graphene devices. The sensitivity of a dense CNT network morphology device is then verified in the aqueous phase.

## 1.2 Thesis Outline

**Chapter 6** explores the non-covalent functionalisation of GFETs and CNT FETs with various linker molecules for insect odorant receptor attachment. The linker molecules tested were 1-pyrenebutanoic acid N-hydroxysuccinimide ester (PBASE) and 1-pyrenebutyric acid (PBA) with 1-Ethyl-3-(3-dimethylaminopropyl)carbodiimide (EDC). Pyrene-NTA and pyrene-biotin were also investigated as other possible linker molecules. The quality of various functionalisation approaches was then explored with various fluorescently-tagged linker molecules and biomolecules. In this process, various potential obstacles to successful biosensor functionalisation were identified.

**Chapter 7** maps out progress made towards the creation of an insect odorant receptor functionalised TFT biosensor for use in a vapour-phase environment. Two different approaches are described that gave rise to working aqueous-phase biosensors. The first functionalisation approach, which used PBASE in methanol, led to irreproducible results when biosensing. Possible factors causing the unreliability of this method were then investigated. A second approach was then designed to avoid the malign influence of any identified factors.

**Chapter 8** outlines the development of a vapour delivery system for characterisation of the insect odorant receptor functionalised TFT biosensors in a vapour-phase environment. The vapour delivery system was upgraded from an existing system to include new mass flow controllers, to have greater control of flow through the system, and off the shelf vapour sensors, to collect vapour flow data that could be used for comparison against biosensor activity. The chapter also describes the design and construction of an electronic interface to monitor and control the components of the vapour delivery system, and calibration of the system.

**Chapter 9** details the use of the vapour delivery system for testing the functionalised biosensors in the vapour phase. First, the flow behaviour of volatile organic vapours through the system was validated using onboard reference sensors. The response of a pristine carbon nanotube device to two volatile compounds is then compared to the response of carbon nanotube devices functionalised using the second functionalisation approach discussed in the previous chapter.

**Chapter 10** summarises the conclusions drawn from this work, and proposes various related studies which can be undertaken to continue the work described in this thesis.



## 2 Vapour Sensing System for Thin-Film Transistor Biosensing

### 2.1 General Overview

Through the adaptation of an existing setup, a custom vapour delivery system was developed to measure the response of field-effect biosensors to vapour. To achieve this goal, the new system needed to meet three requirements:

- The ability to automatically deliver a vapour to an enclosed environment in a controlled manner.
- The ability to collect measurements from a sensor device within that environment.
- The ability to collect data from off-the-shelf reference sensors monitoring the same environment, for comparison with data collected by the novel biosensor.

The existing system had a limited ability to meet the first two requirements, but was not able to take reference measurements of vapour flow. To implement new elements that would enable the system to fulfill all three requirements, a two-step development approach was taken across the course of the thesis. The changes made with each step of the redesign are outlined in Section ??.

Three mass flow controllers (MFC) were used to precisely control and monitor the flow of nitrogen into the system in units of standard cubic centimeters per minute (sccm). The manner in which these controllers were configured in the system is discussed in Section ???. The reference sensors chosen were a photoionisation detector (Ametek Mocon) and relative humidity and temperature indicator (Telaire). The photoionisation detector is able to monitor a wide range of volatile organic compounds, but cannot monitor compounds with an ionisation energy exceeding 10.6 eV. This includes nitrogen, oxygen, carbon dioxide, argon and water [PIDmanual, Ionscience]. Therefore, the photoionisation detector (PID) should not respond to either ambient air or standard nitrogen flow through the detector. As we would also like to monitor the presence of water vapour in the system, we use a relative humidity and temperature indicator (RHI). The operation of these reference sensors is discussed further in Section ??.

## 2.2 Technical Notes

### 2.2.1 Delivery System

Three mass flow controllers (MFCs) and their associated regulators sit in a covered enclosure, seen from the front in Figure ?? (a). The MFCs are used to control the nitrogen flow rate through two delivery lines, the carrier line and dilution line. Each line consists of a mix of stainless steel and flexible PVC tubing, with various Swagelok fittings and valves; these valves include check valves, to ensure there is no vapour backflow. The system is designed so that only one MFC delivers flow through each line. Furthermore, the mass flow controller with a full-scale flow of 500 sccm (standard cubic centimeters per minute) can only be directed through the dilution line, and the mass flow controller with a full-scale flow of 20 sccm can only be directed through the carrier line. The dilution and carrier lines merge at a mixing point about a metre before the device chamber, which contains the device being tested. Flow through the carrier line is bubbled through a volatile compound within a sealed 10 mL Schott bottle (Duran). A three-way valve determines whether the analyte vapour is then carried towards the mixing point or sent to the system exhaust.

### 2.2.2 Reference Sensors

Two reference sensors were added to the vapour delivery setup to compare the response to vapour by the fabricated sensor device with some reference signal. These reference sensors are a Ametek Mocon photoionisation detector and a Telaire relative humidity and temperature indicator. The layout of these reference sensors (and their associated peripherals) relative to the device chamber is shown in Figure ?? (b). These components are on a raised platform directly above the mass flow controller enclosure. Vapour flowing through the device chamber passes into a cylindrical manifold with three outlets. One outlet is the system exhaust, one flows into relative humidity indicator chamber, and one flows into the photoionisation detector. A dial-controlled micro diaphragm pump is used to set the flow rate from the manifold into the photoionisation detector, with a flowmeter used to monitor this flow rate. The electronic integration and programming of the relative humidity and temperature indicator is described in Section ???. The photoionisation detector was connected to a laptop directly via USB, then controlled and monitored using the supplier-provided VOC-TRAQ II software package.

#### Relative Humidity and Temperature Indicator

The relative humidity and temperature indicator used here is a capacitive humidity sensor [TelaireSensor]. It consists of a capacitor with a hygroscopic polymer as the capacitor dielectric. As room temperature water has a much larger dielectric constant than the polymer dielectric, absorption of water by the polymer leads to increased sensor

## 2.2 Technical Notes

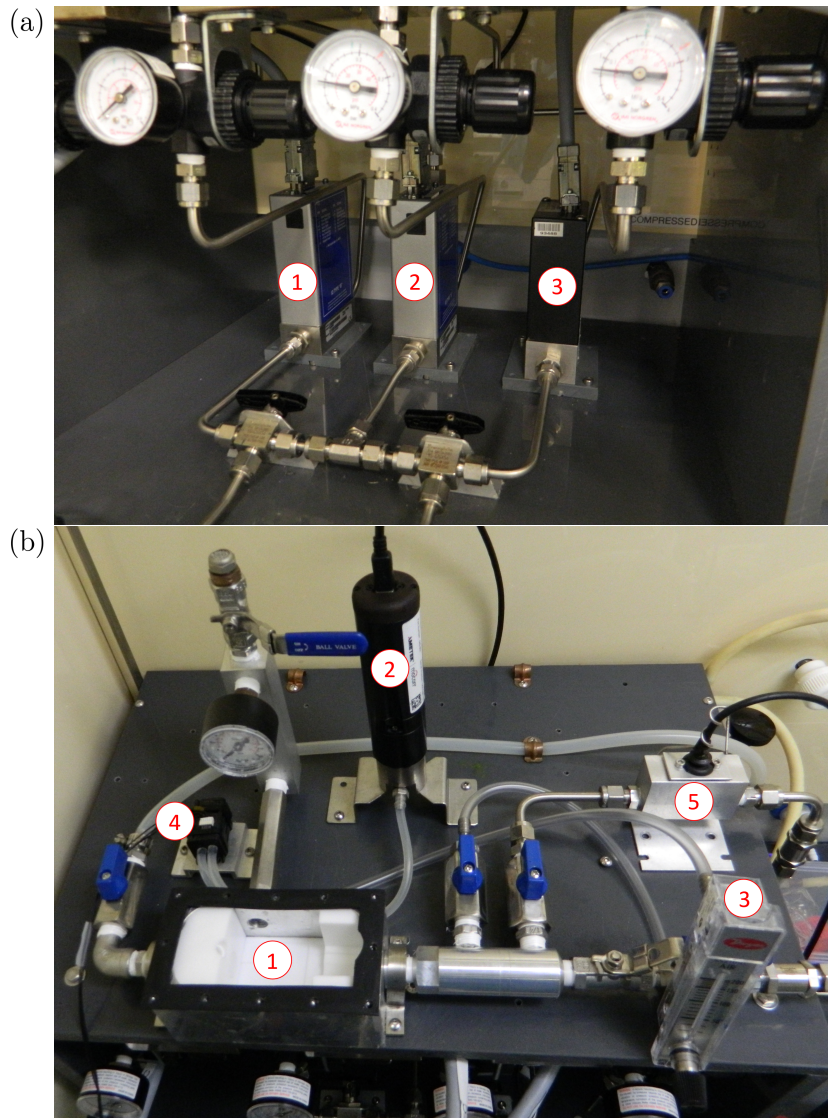


Figure 2.1: The three mass flow controllers (MFCs) of the vapour delivery system are shown in (a), each with a regulator to set the pressure at the MFC inlet. (1) is the 20 sccm full-scale flow MFC, (2) is the 200 sccm full-scale flow MFC, and (3) is the 500 sccm full-scale flow MFC. The device chamber, reference sensors and other chamber peripherals are shown in (b). The components are labelled as follows: (1) Device chamber, (2) Photoionisation detector (PID), (3) Flowmeter from chamber to PID, (4) Micropump from chamber to PID, (5) Relative humidity and temperature monitor.

## 2 Vapour Sensing System for Thin-Film Transistor Biosensing

capacitance [**capacitivesensor**]. The sensor capacitance, corresponding to the amount of moisture absorbed by the polymer and therefore the relative humidity, is then translated by the sensor into a calibrated electronic output. This output is then processed using the hardware and software described in Section ?? to give a value for the relative humidity. The sensor has a quoted relative humidity (RH) accuracy of  $\pm 2.0\%$  when RH is below 80%, and has a quoted temperature accuracy of  $0.5\text{ }^{\circ}\text{C}$  [**Telairesensor**]. The absolute humidity (AH), the mass of water vapour within a set volume, can be calculated in  $\text{gm}^{-3}$  using Equation ??.

$$AH = C \frac{P_W}{T} \quad (2.1)$$

Here,  $C = 2.16679 \text{ gKJ}^{-1}$ ,  $P_W$  is the water vapour pressure (in Pa) and T is the temperature (in K) [**humidityformula**]. For temperatures between  $-20\text{ }^{\circ}\text{C}$  and  $50\text{ }^{\circ}\text{C}$ , water vapour pressure  $P_W$  (in hPa) can be approximated using Equation ??.

$$P_W = RH \times A \times 10^{(mT/(T+T_n))} \quad (2.2)$$

Here, RH is relative humidity, T is temperature in  $^{\circ}\text{C}$ ,  $A = 6.116441 \text{ hPa}$ ,  $m = 7.591386$  and  $T_n = 240.7263\text{ }^{\circ}\text{C}$  [**humidityformula**].

### Photoionisation Detector

A photoionisation detector (PID) can be used to continuously monitor volatile organic compounds by measuring the extent to which vapour molecules passing through the detector can be ionised by incident UV radiation. A small percentage of vapour molecules flowing into the detector diffuse into a sensor cavity. This cavity is bounded on each side by a pair of electrodes. A lamp in the body of the detector radiates UV light through a window into this cavity. The vapour molecules have their outer-most electrons excited and removed when struck with these high-energy photons. The ionised molecules then drift towards the sensor cathode, while free electrons drift towards the sensor anode. This results in a current proportional to the concentration of vapour molecules in the chamber. The current can then be amplified for a signal readout. To be detected, the ionisation energy of the molecules being monitored cannot exceed the energy of the incident UV light. Therefore, molecules of clean air will not be detected. Likewise, volatile organic compounds with high ionisation energy – such as methane – will not be recognised by the PID. Conversely, if the energy required to ionise a volatile of interest is relatively low, the PID will generally show a relatively large response to that volatile [**Ionscience, PIDmanual**].

The Ametek Mocon photoionisation detector lamps used in this work each had a lamp energy of 10.6 eV, with a quoted response time of less than 2 seconds. Photoionisation detectors are designed to sensitively detect within a particular concentration range. PID